

Super-Kamiokande atmospheric neutrinos: Status of subdominant oscillations

G.L. Fogli, E. Lisi, and A. Marrone

*Dipartimento di Fisica and Sezione INFN di Bari
Via Amendola 173, I-70126 Bari, Italy*

Abstract

In the context of the recent (79.5 kTy) Super-Kamiokande atmospheric neutrino data, we concisely review the status of muonic-tauonic flavor oscillations and of the subdominant electron or sterile neutrino mixing, in schemes with three or four families and one dominant mass scale. In the three-family case, where we include the full CHOOZ spectral data, we also show, through a specific example, that “maximal” violations of the one-dominant mass scale approximation are not ruled out yet.

PACS: 14.60.Pq, 13.15.+g, 95.85.Ry

I. INTRODUCTION

The Super-Kamiokande (SK) Collaboration has recently presented an updated set of atmospheric neutrino data for a detector exposure of 79.5 kTy [1]. The corresponding statistics is about twice as large as compared to the one considered in our earlier published analysis of three-flavor mixing [2] and of two-flavor mixing with nonstandard dynamics [3], and is about 12% larger than in our previous analysis of four-family schemes in [4]. In addition, the CHOOZ collaboration presented in [5] final *spectral* data, which we now include in 3ν analyses [6], improving the accuracy of our previous results [2] based on the CHOOZ *total rate* [7].

Therefore, we think it useful to present a concise update of our 2ν , 3ν , and 4ν oscillation studies, performed under the hypothesis of one mass-scale dominance, so as to elucidate the current status and implications of subdominant (electron or sterile) neutrino mixing in *SK*. Finally, we also discuss a specific 3ν example which maximally violates the assumption of one-dominant mass scale.

II. TWO NEUTRINOS

The standard 2ν case of $\nu_\mu \leftrightarrow \nu_\tau$ oscillations can be parametrized by one squared mass difference between two states (ν_1, ν_2),

$$m^2 = |m_2^2 - m_1^2| , \quad (1)$$

and by one mixing angle ψ , describing the flavor content of ν_2 ,

$$|\langle \nu_2 | \nu_\mu \rangle| = s_\psi , \quad (2)$$

$$|\langle \nu_2 | \nu_\tau \rangle| = c_\psi , \quad (3)$$

where $s = \sin$ and $c = \cos$.

Figure 1 shows our 2ν best fit to the latest SK data, reached at $(m^2, \sin^2 2\psi) = (3 \times 10^{-3} \text{ eV}^2, 0.97)$, and corresponding to $\chi^2_{\min} = 38.5$ for $55 - 2$ degrees of freedom—a very good fit.¹ The SK collaboration finds the χ^2 minimum at a slightly different point, $(m^2, \sin^2 2\psi)_{\text{SK}} = (2.5 \times 10^{-3} \text{ eV}^2, 1.0)$ [1]. However, the difference is not statistically significant, since the χ^2 function turns out to be rather flat around the minimum, and the “distance” between our best-fit point and the SK one is only about one unit in $\Delta\chi^2$. Concerning the 2ν bounds on (m^2, ψ) from parameter estimation, they will be discussed later as limits of 3ν and 4ν cases.

The striking evidence in favor of standard $\nu_\mu \leftrightarrow \nu_\tau$ oscillations (Fig. 1) strongly constrains nonstandard explanations. By using the approach described in [3], we parametrize a

¹The overall reduction of χ^2_{\min} with respect to the 2ν (subcase) analysis presented in [4] is mainly due to a better agreement of the latest SK electron distributions with their no-oscillation expectations (especially in the multi-GeV sample).

wide class of scenarios involving nonstandard dynamics through three (free) parameters: an oscillation amplitude α , an overall phase factor β , and an energy exponent n , the standard mass-mixing dynamics being recovered for $n = -1$.

Figure 2 shows the results of such a three-parameter fit in terms of the projection $\chi^2(n)$. The corresponding bounds on n give $n = -1.03 \pm 0.31$ at 90% C.L. ($\Delta\chi^2 = 6.25$ for three free parameters, $N_{\text{DF}} = 3$), in perfect agreement with the standard case. Such results strengthen our previous bounds obtained with smaller (45 kTy) SK statistics ($n = 0.9 \pm 0.4$ [3]), and definitely exclude nonstandard dynamics with integer $n \neq -1$ in the $\nu_\mu \leftrightarrow \nu_\tau$ channel.

III. THREE NEUTRINOS

Oscillations of three neutrinos (ν_1, ν_2, ν_3), under the hypothesis of one mass scale dominance for atmospheric ν 's (equivalent to set $m_1^2 \simeq m_2^2$), are characterized by one squared mass difference,

$$m^2 = m_3^2 - m_{1,2}^2 , \quad (4)$$

(the cases $m^2 > 0$ and $m^2 < 0$ being physically different [8]), and by two mixing angles ($\psi = \theta_{23} \in [0, \pi/2]$ and $\phi = \theta_{13} \in [0, \pi/2]$), describing the flavor content of the state ν_3 ,

$$|\langle \nu_3 | \nu_e \rangle| = s_\phi , \quad (5)$$

$$|\langle \nu_3 | \nu_\mu \rangle| = c_\phi s_\psi , \quad (6)$$

$$|\langle \nu_3 | \nu_\tau \rangle| = c_\phi c_\psi , \quad (7)$$

the pure $\nu_\mu \leftrightarrow \nu_\tau$ case being recovered for $\phi = 0$ (see [2] and references therein).

In order to show the bounds in the mixing parameter space, we used in [2] a triangular representation [9,10], which is basically a linear mapping in the variables $(\sin^2 \psi, \sin^2 \phi)$. Such a representation has the advantage of embedding unitarity by construction, but has the disadvantage of not showing in detail the phenomenologically interesting case of small ϕ . We use here the alternative representation in terms of $(\tan^2 \psi, \tan^2 \phi)$ in logarithmic scale (also introduced in [9,10]), which expands the small ϕ region while preserving octant symmetry (when applicable).

Using SK data only, and assuming $m^2 > 0$, we find the best fit ($\chi^2_{\text{min}} = 38.1$) at $(m^2, \tan^2 \psi, \tan^2 \phi) = (3 \times 10^{-3} \text{ eV}^2, 0.9, 0.01)$. The slight deviation of the best fit mixing from the pure $\nu_\mu \leftrightarrow \nu_\tau$ maximal mixing $[(\tan^2 \psi, \tan^2 \phi) = (1, 0)]$, although intriguing², is—unfortunately—not statistically significant ($\Delta\chi^2 \lesssim 1$). This also implies that there is no significant indication for possible matter effects related to ν_e mixing ($\tan^2 \phi > 0$) in the SK data.

Figure 3 shows the 3ν volume allowed at 90% and 99% C.L. ($\Delta\chi^2 = 6.25$ and 11.36 for $N_{\text{DF}} = 3$, respectively) in the $(m^2, \tan^2 \psi, \tan^2 \phi)$ parameter space, through its projections onto the coordinate planes. The upper limit on $\tan^2 \phi$ ($\lesssim 0.35$ at 90% C.L.) improves the

²There is no reason to have *exactly* $(\tan^2 \psi, \tan^2 \phi) = (1, 0)$.

one found in [2] ($\tan^2 \phi \lesssim 1$ at 90% C.L. from 33 kTy SK data), showing the steady progress of SK in confirming dominant $\nu_\mu \leftrightarrow \nu_\tau$ mixing and in constraining additional ν_e mixing. The 90% C.L. range for m^2 is $(1.6\text{--}7.2) \times 10^{-3}$ eV 2 . The bounds on $\tan^2 \psi$ in Fig. 3 are octant-symmetric only in the 2ν limit $\tan^2 \phi \rightarrow 0$ (as they should), and show a slight preference for ψ in the second octant when $\tan^2 \phi > 0$. Correspondingly, slightly higher values of m^2 are preferred. The (weak) positive correlation between $\tan^2 \phi$ and $\tan^2 \psi$ or m^2 , however, is largely suppressed by the inclusion of CHOOZ data, as we now discuss.

As described in [6], we can now include the CHOOZ reactor spectral data (14 bins minus one adjustable normalization parameter) through a χ^2 statistics reproducing the bounds of the so-called ‘‘CHOOZ analysis A’’ [5]. This improvement provides more accurate bounds in the m^2 region of interest for atmospheric neutrinos. Our best fit to SK+CHOOZ data ($\chi^2_{\min} = 45.7$) is reached at $(m^2, \tan^2 \psi, \tan^2 \phi) = (3 \times 10^{-3}$ eV $^2, 0.75, 0.003)$. Once again, the small deviation of the best fit mixing from $(\tan^2 \psi, \tan^2 \phi) = (1, 0)$ is not statistically significant ($\Delta \chi^2 \lesssim 1$).

Figure 4 shows the projections of the $(m^2, \tan^2 \psi, \tan^2 \phi)$ volume allowed by SK+CHOOZ. By comparing Fig. 3 with Fig. 4, the tremendous impact of CHOOZ on ν_e mixing bounds becomes evident (one order of magnitude difference in the upper bound on $\tan^2 \phi$). As expected, at the small values of $\tan^2 \phi$ allowed by the fit in Fig. 4, both the octant-asymmetry in ψ and the upper limit on m^2 are reduced, and the 90% C.L. range for m^2 becomes $(1.6\text{--}5.3) \times 10^{-3}$ eV 2 .

We have also repeated the fit for the case $m^2 < 0$ (not shown), corresponding to a state ν_3 lighter than $\nu_{1,2}$. For negative m^2 , we get somewhat weaker bounds on $\tan^2 \phi$ ($\lesssim 0.5$ at 90% C.L.) for the fit to SK data only, while the fit to SK+CHOOZ data gives results almost identical to those in Fig. 4. This fact shows that, unfortunately, current atmospheric+reactor data are basically unable to discriminate the sign of m^2 in 3ν scenarios, as it was the case for pre-SK and pre-CHOOZ data [8].

Finally, Fig. 5 shows the SK zenith distributions computed for three representative cases at $\tan^2 \phi = 0.025$ (allowed at 90% C.L. by SK+CHOOZ) and for ψ both maximal ($\tan^2 \psi = 1$) and nonmaximal ($\tan^2 \psi = 1/2$ and 2). Within statistical errors, the 3ν zenith distributions in Fig. 5 are hardly distinguishable from the 2ν one in Fig. 1 (even more so for $m^2 < 0$, not shown), the differences being at most $\sim 1.5\sigma$ in a few bins. Therefore, there is little hope to unambiguously discover $\phi \neq 0$ (i.e., ν_e mixing) from SK atmospheric data in the near future.

IV. FOUR NEUTRINOS

We consider the 4ν (3 active + 1 sterile) scenario described in [4], characterized by a 2+2 mass spectrum with well-separated atmospheric and solar doublets. We also make the simplifying assumption [4] that the atmospheric doublet (ν_3, ν_4) is almost decoupled from ν_e , and that the solar doublet (ν_1, ν_2) is almost decoupled from ν_μ . The dominant mass scale for atmospheric neutrinos is then

$$m^2 = m_4^2 - m_3^2 , \quad (8)$$

and two mixing angles ($\psi = \theta_{23} \in [0, \pi/2]$ and $\xi = \theta_{13} \in [0, \pi/2]$) are sufficient to describe the flavor contents of the state ν_4 ,

$$|\langle \nu_4 | \nu_e \rangle| \simeq 0 , \quad (9)$$

$$|\langle \nu_4 | \nu_\mu \rangle| = s_\psi , \quad (10)$$

$$|\langle \nu_4 | \nu_\tau \rangle| = c_\psi c_\xi , \quad (11)$$

$$|\langle \nu_4 | \nu_s \rangle| = c_\psi s_\xi , \quad (12)$$

the pure $\nu_\mu \leftrightarrow \nu_\tau$ and $\nu_\mu \leftrightarrow \nu_s$ cases being recovered for $s_\xi = 0$ and $s_\xi = 1$, respectively. In such scenario, the cases $m^2 > 0$ and $m^2 < 0$ are not physically different (being equivalent under octant inversion, $\psi \rightarrow \pi/2 - \psi$ [4]), and we take $m^2 > 0$.

Figure 6 shows the bounds obtained by a fit to SK data at 90% and 99% C.L. ($N_{\text{DF}} = 3$) in the parameter space $(m^2, \tan^2 \psi, \tan^2 \xi)$. The best fit point ($\chi^2_{\text{min}} = 38.1$) is reached at $(m^2, \tan^2 \psi, \tan^2 \xi) = (3 \times 10^{-3} \text{ eV}^2, 0.76, 0.1)$ but, once again, the preferred mixing differs from $(\tan^2 \psi, \tan^2 \phi) = (1, 0)$ by less than one unit in $\Delta\chi^2$. Notice that in the $(m^2, \tan^2 \psi)$ plane, the 4ν projected bounds of Fig. 6 are very similar to the 3ν ones in Fig. 4, implying that the current limits on the “ 2ν ” subset of parameters $(m^2, \tan^2 \psi)$ are rather stable even by making allowance for additional ν_s or ν_e mixing.

Concerning the $(\tan^2 \psi, \tan^2 \xi)$ plane in Fig. 6, the upper bounds on $\tan^2 \xi$ indicate that pure $\nu_\mu \leftrightarrow \nu_s$ oscillations ($\tan^2 \xi \rightarrow \infty$) are disfavored as compared with pure $\nu_\mu \leftrightarrow \nu_\tau$ oscillations ($\tan^2 \xi \rightarrow 0$), in agreement with [11,12], although large ν_s mixing is not excluded yet. In particular, the current upper limit from Fig. 6 ($\tan^2 \xi \lesssim 4$ at 90% C.L.) is even slightly *weaker* than the one we found with smaller statistics in [4] ($\tan^2 \xi \lesssim 2$). The reason can be traced to a peculiar feature of the latest UP μ data, namely, the flatness of the muon suppression pattern in the four UP μ bins at $\cos \theta \in [-0.7, -0.4]$, as described in Fig. 7.

Figure 7 shows the SK zenith distributions for three representative 4ν cases with sizable ν_s mixing ($\tan^2 \xi = 1$). As it is well known (and evident from a comparison of Fig. 7 with Fig. 1), additional ν_s mixing for atmospheric neutrinos tends to reduce the muon suppression and, in particular, tends to flatten the normalized UP μ distribution. Although the SK UP μ data do prefer a mean positive slope rather than a flat suppression, the four bins in the zenith range $\cos \theta \in [-0.7, -0.4]$ happen to favor a locally flat distribution. This current feature might be just a statistical fluctuation but, at present, it plays some role in global fits, where it tends to weaken the rejection of “flat” distributions (i.e., of sizable ν_s mixing), as compared with previous UP μ data [4].

The SK Collaboration has also presented additional (preliminary) indication in favor of $\nu_\mu \leftrightarrow \nu_\tau$ mixing coming from statistical ν_τ appearance in selected event samples [1]. It seems possible to isolate an excess of about 100 ± 50 τ -like events, to be compared with standard $\nu_\mu \leftrightarrow \nu_\tau$ expectations of ~ 100 [1]. Taken at face value, such numbers imply an additional $\sim 2\sigma$ evidence ($\Delta\chi^2 \simeq 4$) in favor of pure $\nu_\mu \leftrightarrow \nu_\tau$ ($s_\xi^2 = 0$) as compared with pure $\nu_\mu \leftrightarrow \nu_s$ ($s_\xi^2 = 1$). We have then roughly parametrized the SK “tau appearance” signal by adding a penalty function $\Delta\chi^2 = 4s_\xi^2$ in the 4ν fit. We get an “improved” upper bound $\tan^2 \xi \lesssim 1.5$ at 90% C.L. ($N_{\text{DF}} = 3$), to be compared with $\tan^2 \xi \lesssim 4$ in Fig. 6 (without penalty function). On the one hand, this seems to indicate that there is certainly room to refine current bounds on additional ν_s mixing in SK; on the other hand, our analysis shows that large ν_s mixing (e.g., a fifty-fifty admixture of ν_τ and ν_s at $\tan^2 \xi \simeq 1$) is not yet

excluded at present. Therefore, compatibility with complementary solar neutrino bounds on $\tan^2 \xi$ [13] is still possible, as it was the case for previous SK data [4].

V. TWO, THREE, AND FOUR NEUTRINO SUMMARY

The bounds on dominant and subdominant mixing found in the previous sections can be conveniently summarized in one single plot, as shown in Fig. 8. The left panel shows the bounds on the $(m^2, \tan^2 \psi)$ parameters for pure $\nu_\mu \leftrightarrow \nu_\tau$ mixing (equivalent to our 3ν scheme for $\tan^2 \phi = 0$ or to our 4ν scheme for $\tan^2 \xi = 0$). As discussed before, such bounds are not significantly altered by additional ν_e mixing ($\tan^2 \phi > 0$) or by additional ν_s mixing ($\tan^2 \xi > 0$), and thus they hold also in the global 3ν and 4ν fits with good accuracy. For such reason, the 2ν bounds in the left panel are formally obtained for $N_{\text{DF}} = 3$, so as to match those in the middle and right panels. The middle panel shows the 3ν bounds on additional ν_e mixing ($\tan^2 \phi > 0$), with and without CHOOZ. Finally, the left panel shows the 4ν bounds on additional ν_s mixing ($\tan^2 \xi > 0$). Such synthetic figure represents the main result of our analysis.

VI. TWO MASS SCALES

The analyses in the previous sections are based on the assumption that atmospheric neutrino oscillations are driven by only one mass scale (m^2). This is not necessarily the case, especially if one takes the “solar” squared mass difference in the upper range allowed by the data (see, e.g., [14]), provided that one accepts an averaged or quasiaveraged solar neutrino survival probability [6]. Concerning atmospheric neutrinos, two mass scales in the range $\sim 10^{-3}$ eV 2 were shown to provide acceptable fits to previous SK+CHOOZ data [15]. Here we show, through a specific example, that such possibility is not yet excluded by the latest data.

Let us consider the specific 3ν case shown in Fig. 9, characterized by two equal squared mass differences ($\Delta m_{32}^2 = \Delta m_{21}^2 = 0.7 \times 10^{-3}$) eV 2 , and by mixing angles³ ($\tan^2 \phi, \tan^2 \psi, \tan^2 \omega$) = (0, 1, 2), giving the flavor composition of mass eigenstates shown in the same figure. The spectrum in Fig. 9 might be called “democratic”, since it maximally violates the usual “hierarchical” approximation ($\Delta m_{21}^2 \ll \Delta m_{32}^2$). Notice that ν_e oscillations are driven only by Δm_{21}^2 , which is purposely chosen just below the current CHOOZ bounds [5]. The solar neutrino survival probability is then $P(\nu_e \rightarrow \nu_e) \simeq 1 - \frac{1}{2} \sin^2 2\omega \simeq 5/9 \sim 1/2$, up to small (quasiaveraged [6]) corrections.

Figure 10 shows the SK zenith distributions computed for the democratic scenario in Fig. 9, and corresponding to $\chi^2 = 50.9$ for the fit to SK data only ($\chi^2 = 61.2$ if CHOOZ data are also included). Although such value is significantly higher than in the best-fit 2ν case of Fig. 1, it is still acceptable from the point of view of goodness of fit. All in all, the curves in Fig. 10 provide a globally acceptable “fit-by-eye”, with moderate departures

³In standard notation, $\phi = \theta_{13}$, $\psi = \theta_{23}$, and $\omega = \theta_{12}$.

from the data along the horizontal direction ($\cos \theta \sim 0$) for the MG μ and US μ samples. Therefore, if one accepts an almost constant ($\sim 1/2$) suppression as explanation of the solar neutrino deficit, 3ν scenarios with two comparable mass scales appear to represent a viable possibility in the current atmospheric neutrino phenomenology. Needless to say, the most general analysis of such cases (depending on all the 3ν mass-mixing parameters) would be rather intricated, and is postponed to a future work.

VII. CONCLUSIONS

In the context of the latest (79.5 kTy) SK atmospheric ν data, we have concisely reviewed the status of dominant $\nu_\mu \leftrightarrow \nu_\tau$ oscillations (including the case of nonstandard dynamics, Fig. 2) and of subdominant ν_e and ν_s mixing (in 3ν and 4ν schemes, respectively). In the 3ν case we have applied an improved CHOOZ analysis. The main 2ν , 3ν , and 4ν results are discussed separately and then summarized in Fig. 8. Finally, we have shown (through a specific example) that current atmospheric neutrino data are also compatible with oscillations driven by two comparable mass scales.

ACKNOWLEDGMENTS

This work was supported by INFN and by the Italian MURST within the “Astroparticle Physics” project.

REFERENCES

- [1] Super-Kamiokande presentations in winter conferences: C. McGrew in *Neutrino Telescopes 2001*, 9th International Workshop on Neutrino Telescopes (Venice, Italy, March 2001), to appear; T. Toshito in *Moriond 2001*, XXXVI Rencontres de Moriond on Electroweak Interactions and Unified Theories (Les Arcs, France, March 2001), to appear.
- [2] G.L. Fogli, E. Lisi, A. Marrone, and G. Scioscia, Phys. Rev. D **59**, 033001 (1999).
- [3] G.L. Fogli, E. Lisi, A. Marrone, and G. Scioscia, Phys. Rev. D **60**, 053006 (1999).
- [4] G.L. Fogli, E. Lisi, and A. Marrone, Phys. Rev. D **63**, 053008 (2001).
- [5] CHOOZ Collaboration, M. Apollonio *et al.*, Phys. Lett. B **466**, 415 (1999).
- [6] G.L. Fogli, E. Lisi, and A. Palazzo, hep-ph/0105080.
- [7] CHOOZ Collaboration, M. Apollonio *et al.*, Phys. Lett. B **420**, 397 (1998).
- [8] G.L. Fogli, E. Lisi, D. Montanino, and G. Scioscia, Phys. Rev. D **55**, 4385 (1997).
- [9] G.L. Fogli, E. Lisi, and G. Scioscia, Phys. Rev. D **52**, 5334 (1995).
- [10] G.L. Fogli, E. Lisi, and D. Montanino, Phys. Rev. D **54**, 2048 (1996).
- [11] Super-Kamiokande Collaboration, S. Fukuda *et al.*, Phys. Rev. Lett. **85**, 3999 (2000).
- [12] MACRO Collaboration, talk by B.C. Barish in *Neutrino 2000*, Proceedings of the 19th International Conference on Neutrino Physics and Astrophysics, edited by J. Law, R.W. Ollerhead, and J.J. Simpson, Nucl. Phys. B (Proc. Suppl.) **91**, 141 (2001).
- [13] C. Giunti, M.C. Gonzalez-Garcia, and C. Peña-Garay, Phys. Rev. D **62**, 013005 (2000); M.C. Gonzalez-Garcia and C. Peña-Garay, Phys. Rev. D **63**, 073013 (2001).
- [14] S. Choubey, S. Goswami, N. Gupta, and D.P. Roy, hep-ph/0103318.
- [15] A. Strumia, J. of High Energy Physics, **04** 26 (1999).

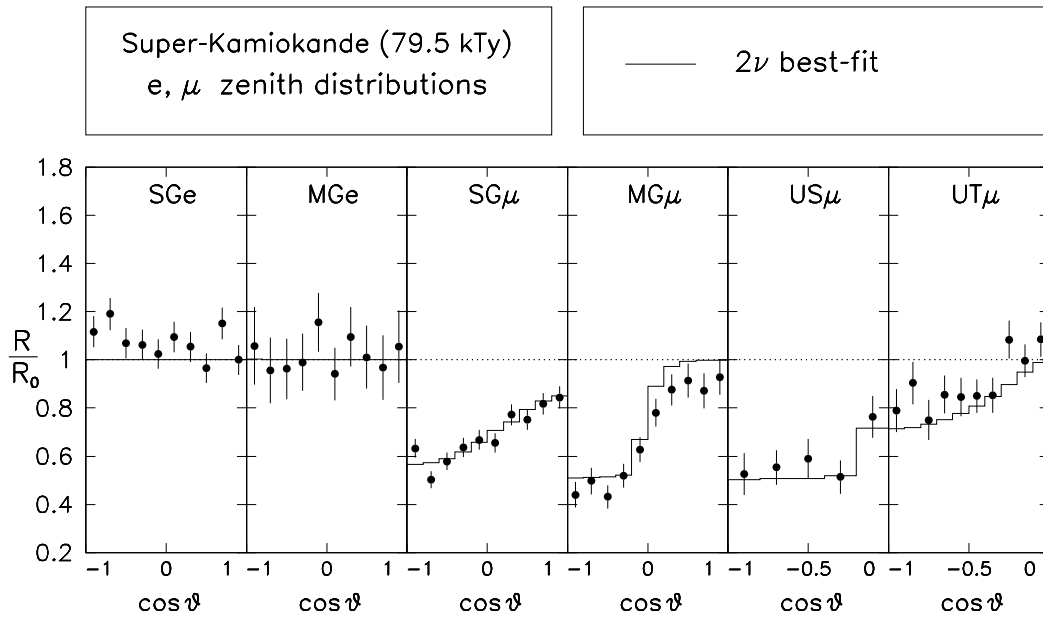


Fig. 1. Super-Kamiokande zenith distributions (79.5 kTy [1]) used in the analysis, normalized to no-oscillation expectations. The data set includes sub-GeV electrons (SGe, 10 bins), multi-GeV electrons (MGe, 10 bins), sub-GeV muons (SG μ , 10 bins), multi-GeV muons (MG μ , 10 bins), upward stopping muons (US μ , 5 bins), and upward through-going muons (UT μ , 10 bins), for a total of 55 data points. The error bars are statistical only ($\pm 1\sigma$); systematic (correlated) uncertainties are treated as in [2]. The solid line is our best fit for 2ν oscillations ($\chi^2 = 38.5$).

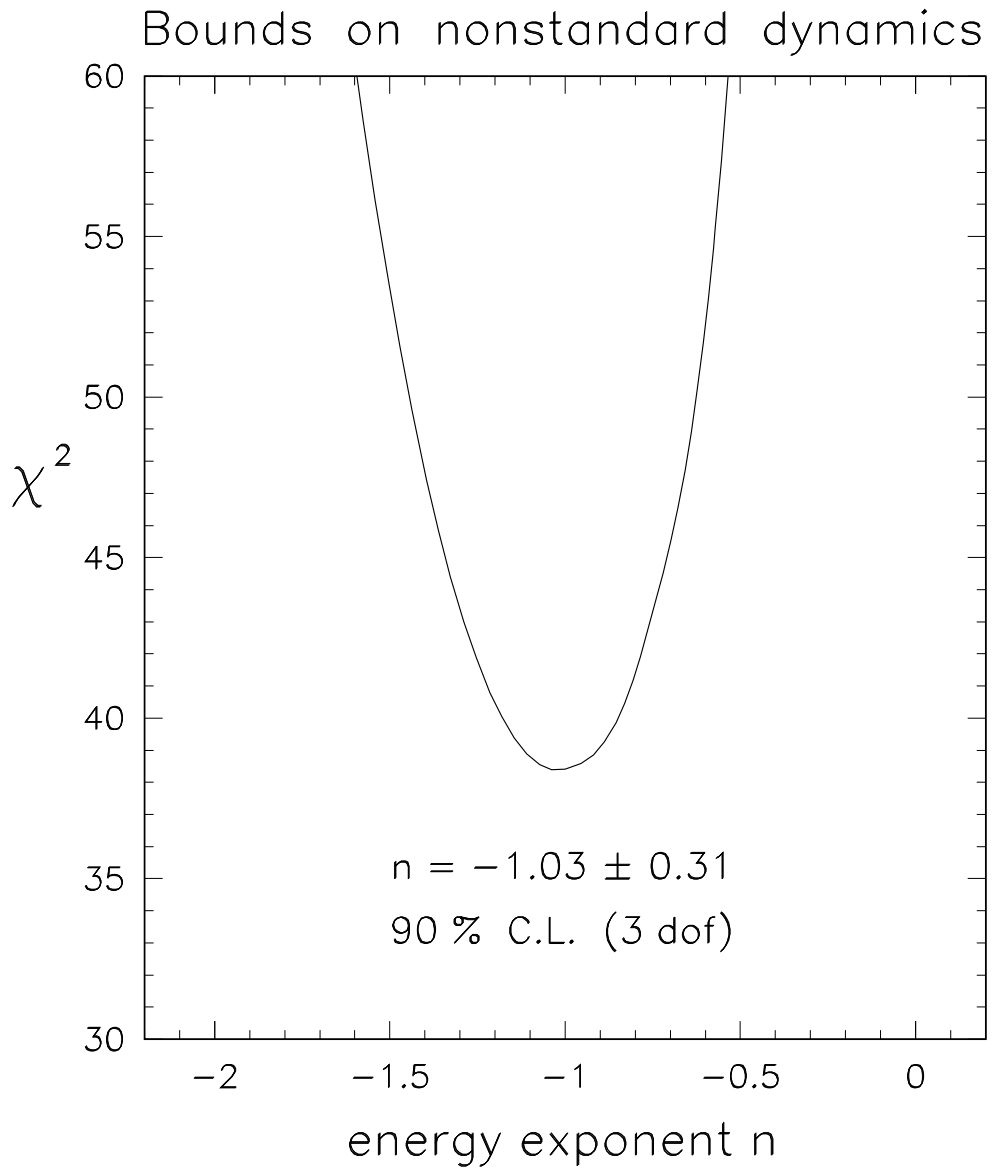


Fig. 2. Dependence of the χ^2 function on the neutrino energy exponent n , assuming an oscillation phase proportional to E^n , with unconstrained factors for the overall phase and amplitude. The only integer n compatible with the SK data is $n = -1$, corresponding to standard mass-mixing dynamics.

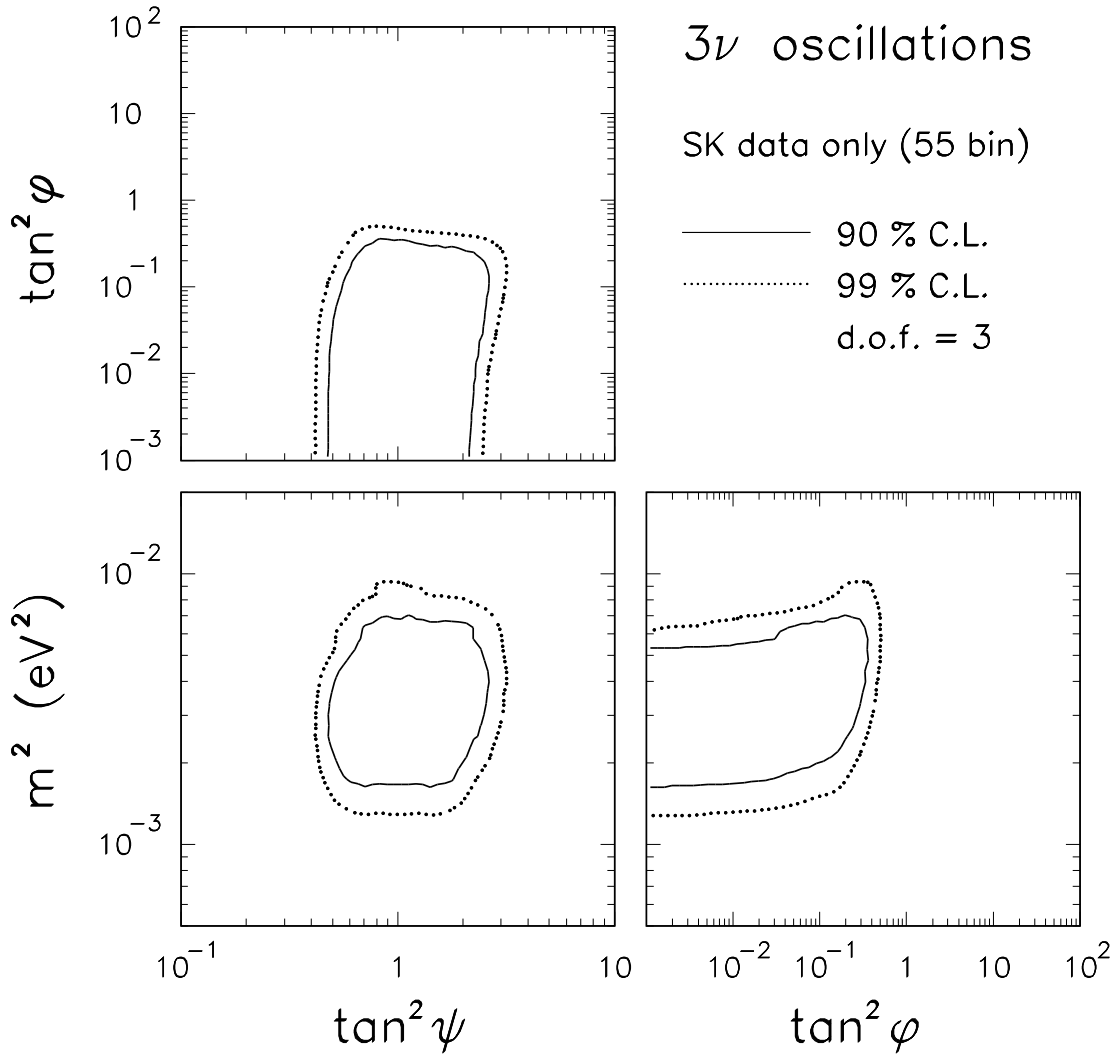


Fig. 3. Projections of the regions allowed in the 3ν parameter space (m^2 , $\tan^2 \psi$, $\tan^2 \phi$) at 90% and 99% C.L. ($\Delta\chi^2 = 6.25$ and 11.36 for $N_{\text{DF}} = 3$) onto the coordinate planes. The fit includes SK data only (79.5 kTy). The pure 2ν case of $\nu_\mu \leftrightarrow \nu_\tau$ oscillations is recovered for $\tan^2 \phi \rightarrow 0$. Nonzero values of ϕ parametrize ν_e mixing.

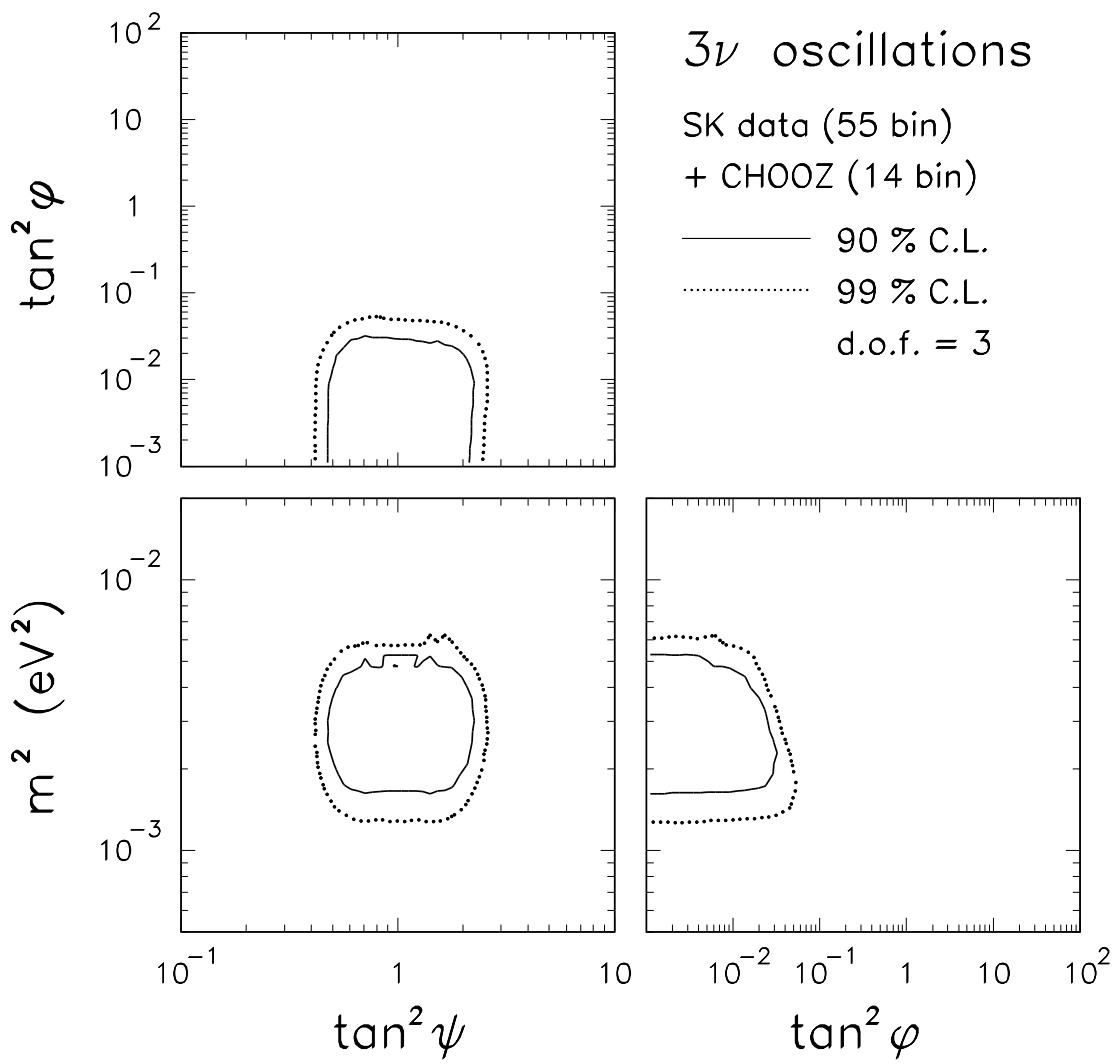


Fig. 4. As in Fig. 3, but including final CHOOZ positron spectra [5] (14 data points minus one adjustable normalization factor).

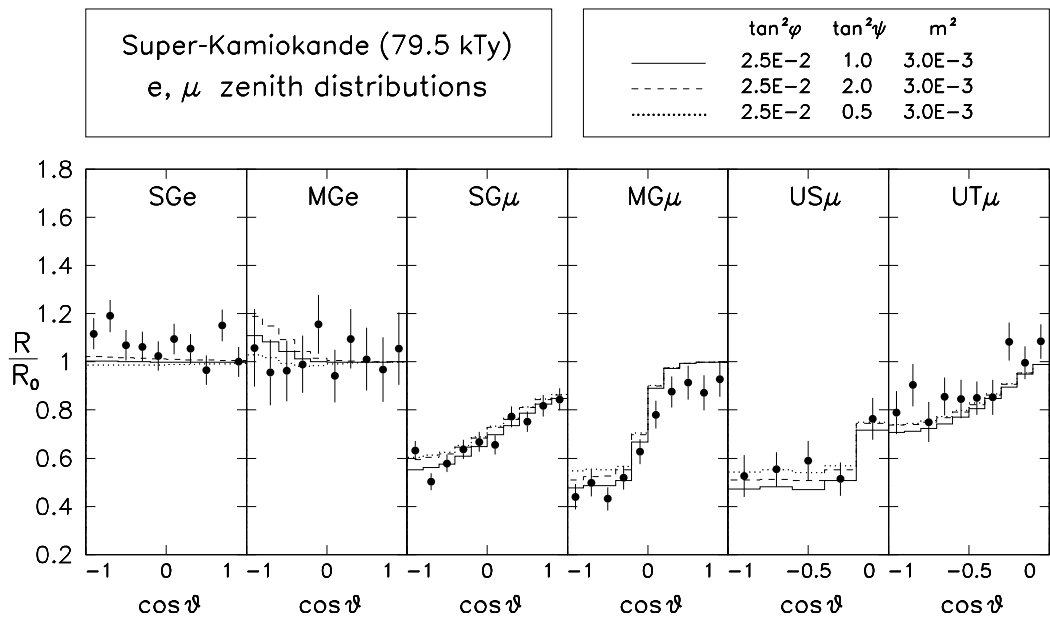


Fig. 5. Zenith distributions for three representative 3ν cases with $\tan^2\phi = 2.5 \times 10^{-2}$, allowed at 90% C.L. by SK+CHOOZ. Notice the distortion of the MGe distribution. Such distortion would be somewhat smaller for negative $m^2 = -3 \times 10^{-3}$ eV 2 (not shown).

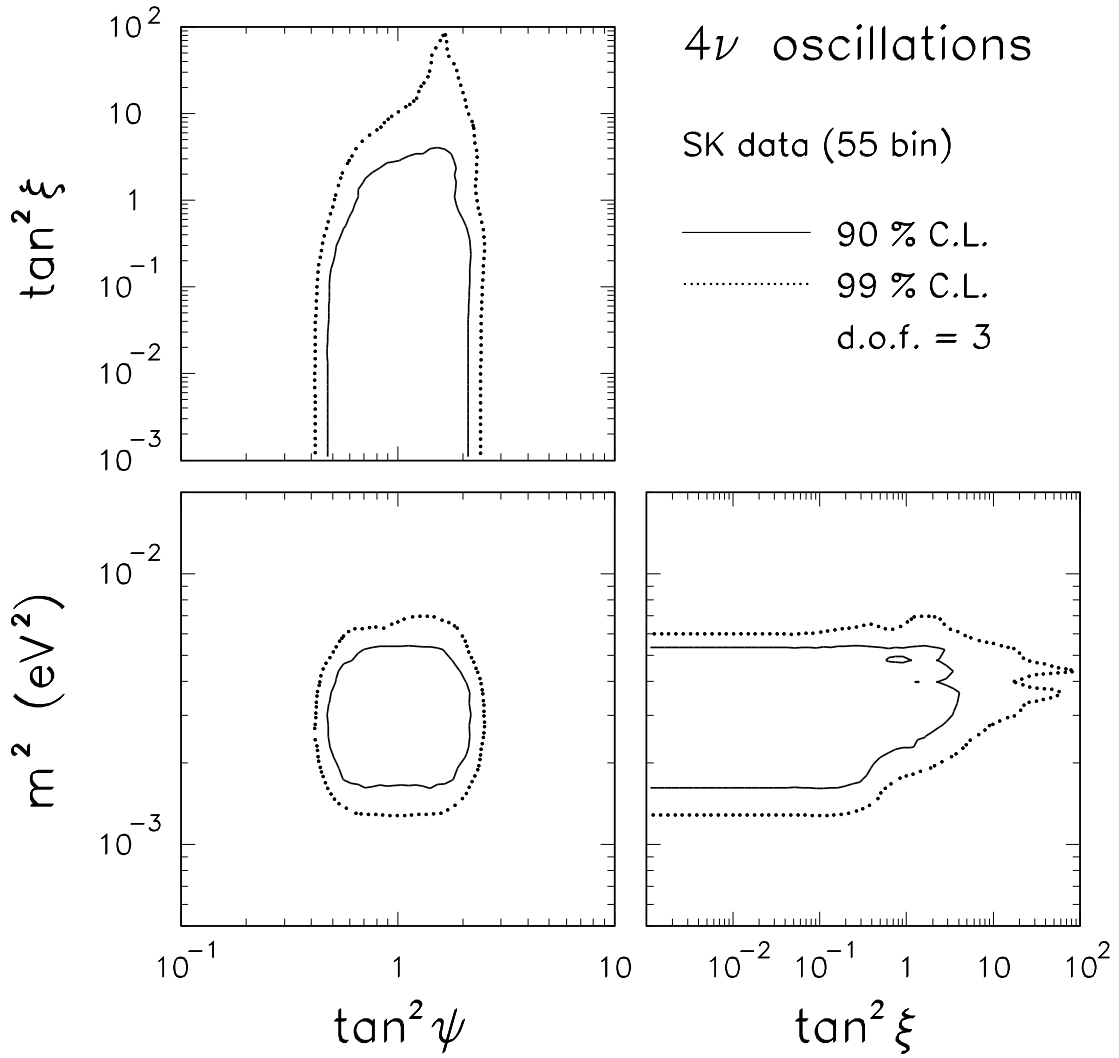


Fig. 6. Projections of the regions allowed in the 4ν parameter space ($m^2, \tan^2 \psi, \tan^2 \xi$) at 90% and 99% C.L. ($\Delta\chi^2 = 6.25$ and 11.36 for $N_{\text{DF}} = 3$) onto the coordinate planes. The fit includes SK data only (79.5 kTy). The pure $\nu_\mu \leftrightarrow \nu_\tau$ case ($\tan^2 \xi \rightarrow 0$) is clearly preferred over the pure $\nu_\mu \leftrightarrow \nu_s$ case ($\tan^2 \xi \rightarrow \infty$). However, sizable ν_s mixing [$\tan^2 \xi \sim O(1)$] is allowed in addition to $\nu_\mu \leftrightarrow \nu_\tau$ oscillations.

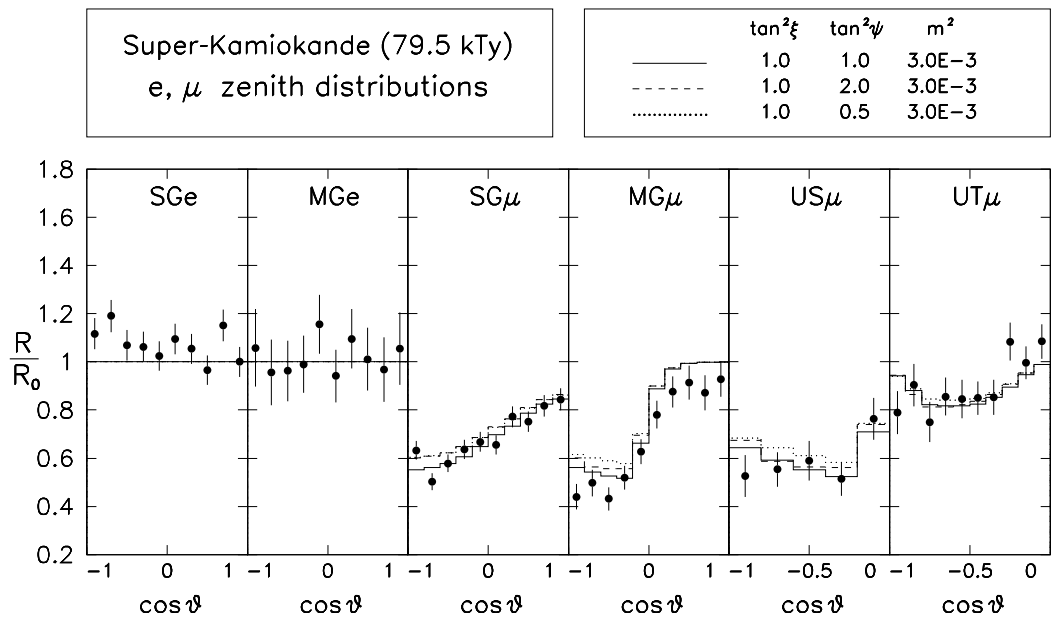


Fig. 7. Zenith distributions for three representative 4ν cases with sizable ν_s mixing ($\tan^2 \xi = 1$), allowed at 90% C.L. by SK data. Notice the reduced suppression in the muon samples, as compared with pure $\nu_\mu \leftrightarrow \nu_\tau$ mixing in Fig. 1.

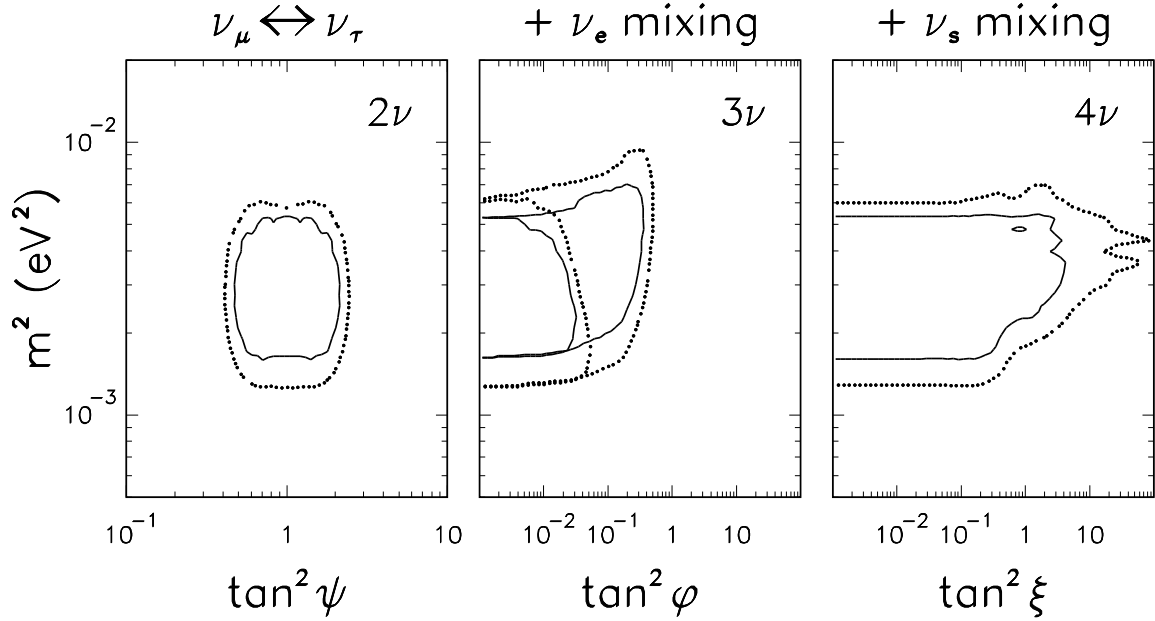


Fig. 8. Summary of 2ν , 3ν , and 4ν bounds at 90% and 99% C.L. on the mass-mixing parameters from SK data. Left panel: Bounds on $(m^2, \tan^2 \psi)$ for pure $\nu_\mu \leftrightarrow \nu_\tau$ mixing (i.e., for $\tan^2 \phi = 0 = \tan^2 \xi$). Middle panel: Bounds on additional ν_e mixing (parametrized by $\tan^2 \phi > 0$) in 3ν scenarios, both without CHOOZ (see also Fig. 3) and with CHOOZ (see also Fig. 4). Right panel: Bounds on additional ν_s mixing (parametrized by $\tan^2 \xi > 0$) in 4ν scenarios (see also Fig. 6). All the bounds are derived for $N_{\text{DF}} = 3$, including those in the left panel.

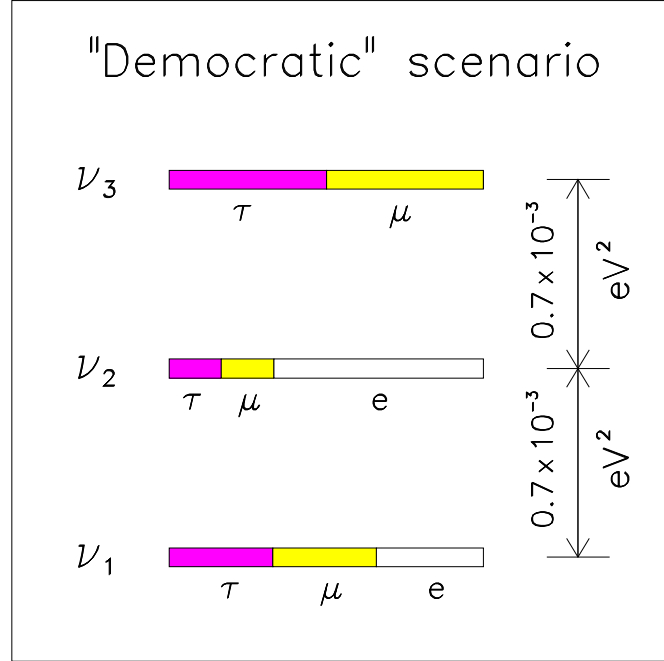


Fig. 9. A “democratic” (i.e., nonhierarchical) 3ν scenario with two equal squared mass differences ($\Delta m_{32}^2 = \Delta m_{21}^2 = 0.7 \times 10^{-3} \text{ eV}^2$) and with $(\nu_e, \nu_\mu, \nu_\tau)$ flavor content as follows: $(1/3, 1/3, 1/3)$ for ν_1 , $(1/6, 1/6, 1/6)$ for ν_2 , and $(0, 1/2, 1/2)$ for ν_3 . Notice that ν_e disappearance is driven only by Δm_{21}^2 (just below the CHOOZ sensitivity [5]), and gives $P(\nu_e \rightarrow \nu_e) \simeq 5/9$ for solar neutrinos (up to small quasiaveraged oscillation corrections).

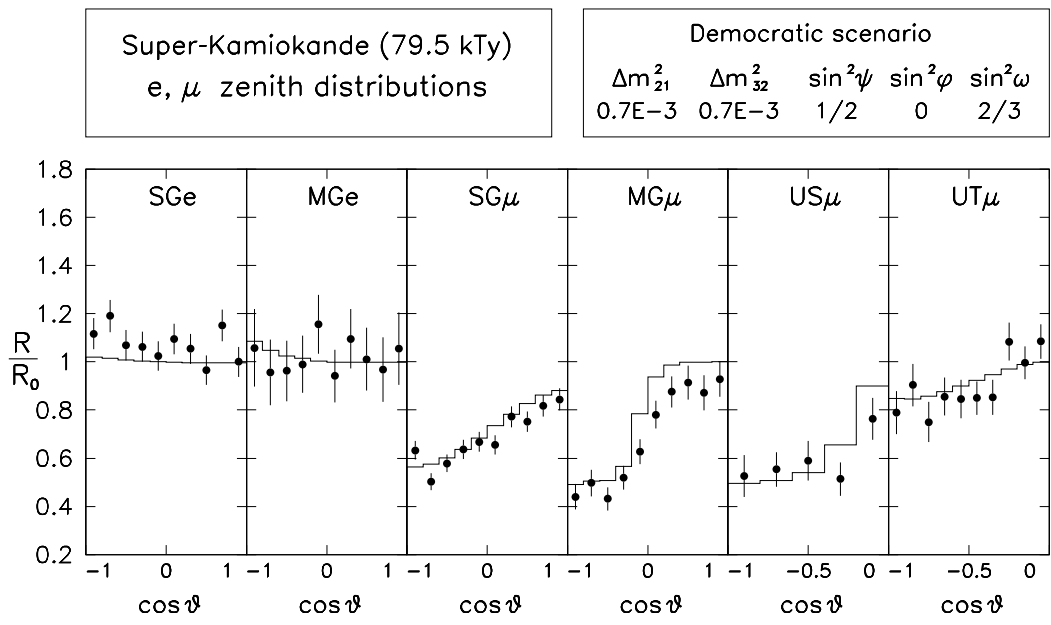


Fig. 10. Zenith distributions for the democratic scenario in Fig. 9, giving $\chi^2 = 50.9$ for the fit to SK data ($\chi^2 = 61.2$ for the fit to SK+CHOOZ).